ISSN 1392–1320 MATERIALS SCIENCE (MEDŽIAGOTYRA). Vol. XX, No. X. 2022

Laser Cladding of Ni-Co-W Composite Coating on Stainless Steel to Enhance Wear Resistance

Linlin ZHANG [1, 2], Dawei ZHANG [3 *]

[1] *Nanjing Vocational University of Industry Technology, Nanjing 210046, Jiangsu Province, China*
[2] *Nanjing University of Aeronautics and Astronautics, Nanjing 211106, Jiangsu Province, China*
[3] *College of Mechanical & Electrical Engineering, Wenzhou University, Wenzhou 325035, Zhejiang Province, China*

crossref http://dx.doi.org/10.5755/j02.ms.28686

Received 23 March 2021; accepted 08 June 2021

Ni-Co-W composite coatings modified by different contents of Co-based alloy powder in the Ni-based alloy with 35 wt.% WC (Ni35WC) were deposited on stainless steel by laser cladding. The influence of compositional and microstructural modification on the wear properties has been comparatively investigated by XRD, SEM, and EDS techniques. It was found that the austenite dendrites in the modified coating adding 50 wt.% Co-based alloy were refined and a lot of $Cr_{23}C_6$ or $M_{23}(C, B)_6$ compounds with fine lamellar feature were formed around austenitic grain boundaries or in the intergranular regions. The contribution of element Co to the modification of Ni35WC coating is that it cannot only promote the formation of more hard compounds to refine austenite grains, but also refine the size of precipitates, and change the phase type of eutectic structure as a result of disappeared Cr boride brittle phases. A noticeable improvement in wear resistance is obtained in the Ni35WC coating with 50 wt.% Co-based alloy, which makes the wear rate decreased by about 53 % and 30% by comparison to that of the substrate and the Ni35WC coating, respectively. It is suggested that the improvement is closely related to the composite coating being strengthened owing to the increase of coating hardness, formation of a fine-grained microstructure caused by Co, and fine hard precipitate phases in the eutectic structure.
Keywords: wear resistance, laser cladding, Ni-based alloy, Ni-Co-W composite coating, microstructural refinement.

1. INTRODUCTION

Stainless steel components with a lower hardness are difficult to use in harsh environments such as corrosive wear, particle erosion, and strong dry friction wear [1 – 4]. The selection of appropriate laser-clad materials can significantly improve their erosion resistance [5], corrosion resistance [6, 7], and wear resistance [8]. However, defects such as crack and pores in the cladding layer are a major problem restricting its industrial use [9], especially when cladding hard wear-resistant coatings such as Ni-base alloy [10, 11] and Ni-base superalloy [12, 13] with a high γ' volume fraction are more likely to cause transverse penetration cracks and solidification cracking of the coating. The causes of crack formation in the cladding layer are mainly related to the high thermal stress caused by laser rapid heating and fast cooling, some hard phases exist in the coating to increase the brittleness and segregation of some low melting point intermetallic compounds at the grain boundary [9].

Due to both the strength and toughness of the fine grain structure, grain refinement is considered to improve the solidification cracking resistance and mechanical properties of welds [14]. Some studies have been reported in this area, for example, the study by Foroulis [15] on the sliding wear behavior of Ni-base H40 alloy hardfaced on 316ss also indicated that the hardfacing alloys should be hard and ductile to have good anti-wear properties. Furthermore, studies [16 – 18] on the non-surface hardened alloys showed that the strength and toughness of the alloys could be greatly improved by obtaining fine grain structure. Hou et al. [19] reported that Mo added to the Ni-based alloy could refine the Ni-rich dendrites and change the Cr-rich compounds in the interdendritic region from plate-like to net-like. The studies by Shaikh Asad Ali Dilawary et al. [20] and Alhattab A.A.M et al. [21] on Mo-modified Ni-based alloys also confirmed that Mo has the effect of refining microstructure, improving the hardness and wear resistance. The study by Hemmati et al. [22] on the cracking tendency of laser deposition layer with Zr and Nb-modified Ni-base commonly 69 alloy showed that the addition of Zr does not cause any microstructural refinement, while the addition of Nb considerably refines the scale of Cr borides without affecting the hardness of the alloy, but this refinement does not reduce the cracking tendency of the deposits. Another study by Hemmati et al. [23] expounded a toughening mechanism of laser deposited coatings formed by the Nb-modified Ni-based alloy to refine microstructure. The study by Liang et al. [24] on the Ni-based alloy coating modified with rare earth showed that there were no cracks and pores in the coatings contained 4 %CeO_2, 5 % Y_2O_3, and 5 % La_2O_3 respectively, and the microstructure was refined, but the study did not mention the effect on properties. Zhao et al. [25] reported that the microstructure of Ni-based coating with nanometer La_2O_3 addition was refined because of La segregates in inter dendrite and thus limiting secondary dendrites growth and ripening, the hardness and wear resistance of the coating were improved in comparison with the base steel.

The above recent studies indicate that the fine-grained structure obtained by modifying the composition of the alloy can enhance the solidification cracking resistance.

* Corresponding author. Tel.: +86-13329305863.
E-mail address: *00131014@wzu.edu.cn* (D.W. Zhang)

However, so far, only a few beneficial alloying elements, such as Mo, Zr, Nb, and rare earth, can be used for compositional modification of Ni-based alloys, among which Nb can refine the microstructure but cannot reduce the cracking tendency, which shows that these modified elements have different functions in inhibiting cracking, refining microstructure and improving properties, thus relevant refining mechanism of modification needs to be further studied. In this study, Co-based alloy powder was used as modified material to modify the composition and microstructure of Ni-based alloy with 35 wt.% WC (Ni35WC). A fine cellular-dendritic structure with particle size of about 3 – 10 μm in the modified coatings was obtaind by the optimized laser process parameters. There were no cracks in the coatings, and the hardness and wear resistance were improved. This work aims to investigate the effects of compositional and microstrctural changes in the modified coatings on the hardness and dry sliding wear properties of Ni35WC coating. Based on the experimental results, the possible mechanism by compositional and microstructural modification used for the Ni35WC alloy was discussed.

2. EXPERIMENTAL PROCEDURE

Stainless steel test blocks with a hardness of 220 – 230 HV and a size of 50 × 25 × 10 mm were selected as the substrate material used for laser cladding. A composite powder composed of Ni35WC and a certain amount of Co-based alloy with a particle size of 10 – 30 μm was selected as the cladding material. The particle size of Ni-based alloy powder is 10 – 30 μm, and its morphology is nearly spherical in SEM. The composition of the cladding sample is similar to that of SUS201 steel. Table 1 shows the nominal composition of the Ni-based and Co-based alloys as well as the substrate. Three kinds of composite powders Ni35WC, Ni35WC + 30 wt.% Co-based alloy, and Ni35WC + 50 wt.% Co-based alloy was used as the laser coating material, respectively.

A continuous wave CO_2 laser with nominal power of 5kW was used for laser cladding treatment. A laser power of 2.5 – 3.5 kW, a beam diameter of 3 – 5 mm, a scanning speed of 3.0 – 8.0, mm·s^{-1} and an overlap ratio of 0.5 were selected as laser process parameters.

Dry sliding friction and wear tests of different laser cladding samples and substrates were carried out using pin-on-disc friction and wear tester at room temperature. The grinding disc is made of a hard alloy (WC-8 % Co) with a hardness of about HV1050. The sliding speed of 1.432ms^{-1} with a normal load of 100 N and sliding distance of 50 – 1200 m were selected as the technological parameters of the dry friction and wear test. Each data point was derived from the average of at least three samples.

The microstructure and composition of the composite coatings were analyzed by a Zeiss optical microscope and a JEOL JSM-6700F field emission scanning electron microscopy (SEM) equipped with an Oxford INCA7421 type energy dispersive X-ray spectrometer (EDS), and the phase analysis of cladding layers was completed emplying of a Rigaku D/max-IIIA type X-ray diffractometer (XRD). A Vickers hardness tester was used to measure the hardness distribution curve of the cross-section in the coating, and a test load of 0.2 kg and a loading time of 15 s were selected as the test parameters.

3. RESULTS

Macrostructural features of the laser-clad composite coatings are shown in Fig. 1. It is seen that the structure of the three coatings has obvious cellular-dendritic characteristics. Under the same laser processing parameters, the grain size of cellular dendrite in the coating with the Co-based alloy is smaller than that without the Co-based alloy. With the additive amount of Co-based alloy powder increased to 50 wt.%, the morphology of a like fishbone appears in the macrostructure, and its cellular dendrite structure is much finer and denser than that of the other coatings, as shown in Fig. 1 c. SEM micrograph of a greater magnification in Fig. 2 further shows the difference of microstructures between the coatings with and without Co-based alloy.

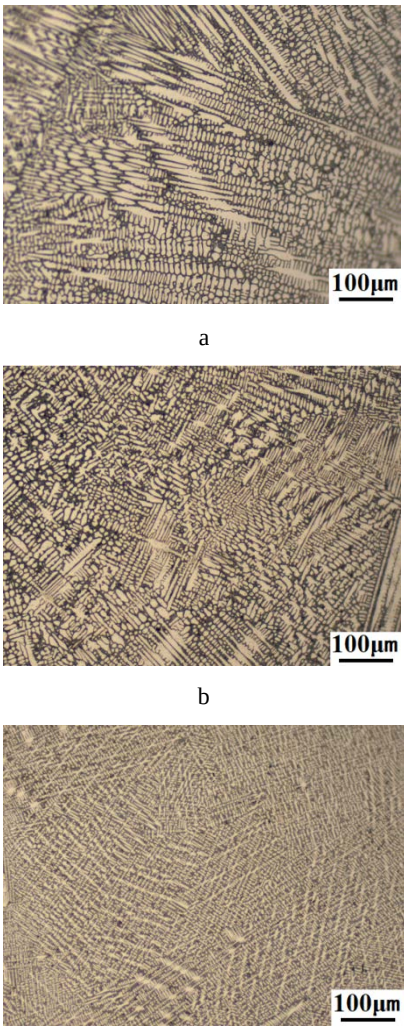

Fig. 1. Macrostructure of laser-clad coatings: a – Ni35WC; b – Ni35WC + 30 wt.% Co-based alloy; c – Ni35WC + 50 wt.% Co-based alloy

It can be seen from Fig. 2 that the microstructure of Ni35WC coating is mainly composed of cellular austenite dendrites and a lot of block and lath-shaped Cr-rich phases in the interdendritic region, and the size of the cellular

grains is about 8 μm long and 3 μm in diameter (see Fig. 2 a).

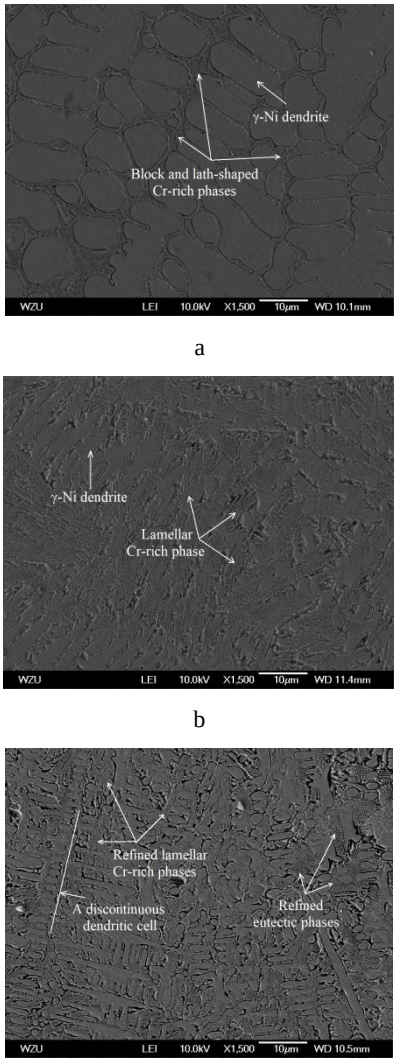

Fig. 2. SEM micrographs showing the difference of microstructures between the coatings with and without Co-based alloy: a – Ni35WC; b – Ni35WC + 30 wt.% Co-based alloy; c – Ni35WC + 50 wt.% Co-based alloy

In the coating added 30 wt.% Co-based alloy powder, the microstructure of coating is refined, and both length and diameter of cellular austenite grains are reduced. The microstructural features are mainly composed of fine cellular austenite dendrites and plenty of lamellar Cr-rich phases in the interdendritic region (see Fig. 2 b). With increasing additive amount of Co-based alloy powder to 50 wt.%, the microstructure of the coating is further refined. Some fine compounds generated in the eutectic structure make the continuity of dendrite growth be broken, which resulted in the formation of many discontinuous cellular austenite grains with the length of about 2 – 5 μm and the diameter of about 1μm during solidification. Moreover, the lamellar Cr-rich phase is further refined, and some finer phases appear in the eutectic structure of the coating, as shown in Fig. 2 c.

The XRD curves of laser cladding Ni35WC, Ni35WC + 30 wt.% Co-based alloy and Ni35WC + 50wt.% Co-based alloy coatings are shown in Fig. 3. The existence of γ-Ni, $M_{23}C_6$, CrB, Cr_2B, M_7C_3, and a small amount of Ni_3B phases in the original single Ni-based alloy powder was confirmed by XRD analysis [26]. After adding 35 wt.% WC into a single Ni-based alloy, lots of γ-Ni austenite, undissolved WC, $Cr_{23}C_6$, Ni_3B, and Cr_5B_3 are detected in the composite coating, as shown in Fig. 3 a.

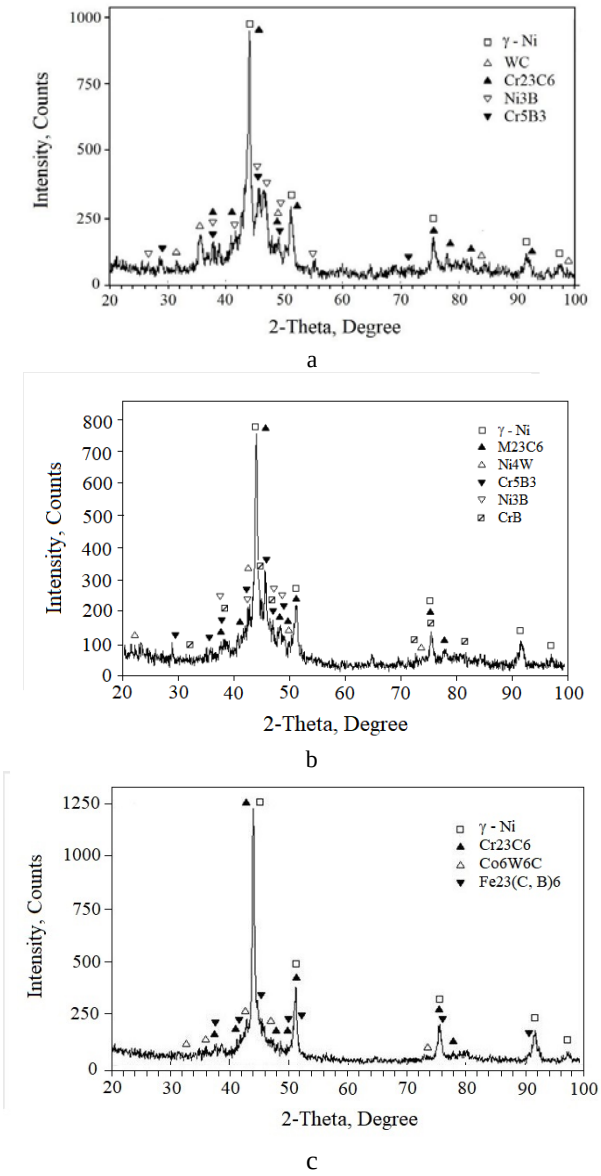

Fig. 3. XRD patterns of laser-clad coatings: a - Ni35WC; b - Ni35WC + 30wt.% Co-based alloy; c - Ni35WC + 50wt.% Co-based alloy

The absence of the Cr_7C_3 is due to its complete dissolution in the melted pool during laser processing. In the Ni35WC coating added 30 wt.% Co-based alloy powder,γ-Ni austenite, $M_{23}C_6$, Ni_4W, Cr_5B_3, Ni_3B, and CrB are detected by XRD (see Fig. 3 b), while WC was completely dissolved, and part of W reacted with Ni to form Ni_4W compound. There are more chromium-rich phases in the coating due to the existence of more chromium-boron compounds. Combined with the SEM image in Fig. 2 b, it can be seen that the lamellar structure in the interdendritic region of the coating should be mainly Cr-rich compounds. With the addition of Co-based alloy powder up to 50 wt.%, there is a large change in the phase component of the

coating. The γ-Ni solid solution, $Cr_{23}C_6$, Co_6W_6C, and $Fe_{23}(C, B)_6$ are detected (see Fig. 3 c), while the WC particle phase, nickel-boron, and chrome-boron compounds were completely dissolved. Part of W combines with Co and C to form the Co_6W_6C compound. Combined with the SEM morphology of Fig. 2 c, it can be seen that the eutectic structure refined in the interdendritic region should mainly contain the above three compounds.

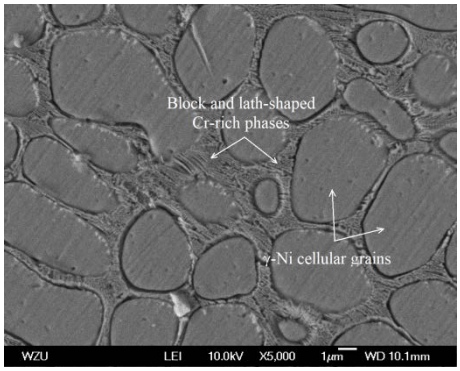

a

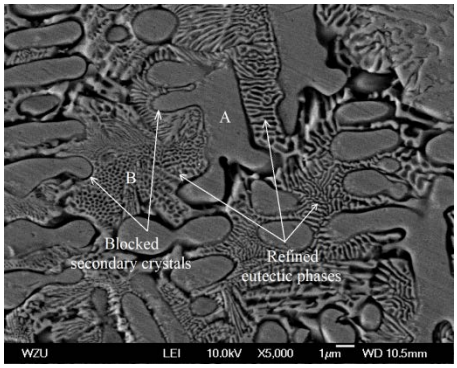

b

Fig. 4. SEM micrographs of the laser-clad coatings showing the different lamellar structures: a – Ni35WC; b – Ni35WC + 50 wt.% Co-based alloy

Fig. 4 shows the SEM micrographs with high magnification in laser-clad coatings of Ni35WC and Ni35WC + 50 wt.% Co-based alloy. It can be seen from the figure that the microstructure of Ni35WC coating shows up coarse austenite cellular grains, and there are block and lath-shaped Cr-rich phases among the cellular grains, as shown in Fig. 4 a, while the coating with 50 wt.% Co-based alloy has diversified microstructure characteristics. In comparison, the amount and density of the fine lamellar structure in the coating with Co-based alloy are significantly more than those without Co-based alloy. These fine lamellar eutectic phases are densely distributed around the austenitic grain boundary or in the intergranular regions, which significantly inhibits the secondary crystal growth of some austenitic dendrites. The block and lath-shaped Cr-rich phases in the Ni35WC coating and lamellar Cr-rich phase existing in the interdendritic region of coating added 30 wt.% Co-based alloys are further refined, and some of the finer network and honeycomb-shaped compounds are formed in the coating with 50 wt.% Co-based alloy, as shown in Fig. 4 b.

EDS analysis was performed for the micro area composition. The micro-area A marked in Fig. 4 b represents the γ-Ni cellular dendrites, and the micro-area B represents the interdendritic eutectic structure. The analysis shows that the rapid heating and cooling of laser beam make plenty of Cr, Fe, W and other elements dissolve in γ-Ni solid solution. No Co element is detected in the cellular austenite dendrite of the coating added Co-based alloy powder, while lots of Cr, Fe, Co, and W elements are found in the interdendritic eutectic structures, as shown in Fig. 4 b and Table 2. Combined with XRD and SEM analysis, $Cr_{23}C_6$, Co_6W_6C and $Fe_{23}(C, B)_6$ compounds constitute the eutectic with γ-Ni austenite, and the compounds should be mainly distributed in the eutectic structure among the γ-Ni dendrites. In addition, by comparing the XRD peak intensity in Fig. 3, it can be seen that the diffraction peak intensity of $Cr_{23}C_6$ in the coating with 50 wt.% Co-based alloy is significantly higher than that of this compound in the Ni35WC alloy, indicating the more $Cr_{23}C_6$ and $M_{23}(C, B)_6$ compounds to be formed in the composite coatings. The dispersion and uniform distribution of these hard compounds in the fine-grained dendrite structure should be very helpful to improve the hardness and wear resistance of the clad layer.

Table 2. EDS analysis of micro-area A and B marked in Fig. 4 b (wt.%)

Element	Cr	Fe	Ni	Co	W
Area A	21.55	37.04	12.54	–	28.87
Area B	32.88	13.58	–	6.95	46.59

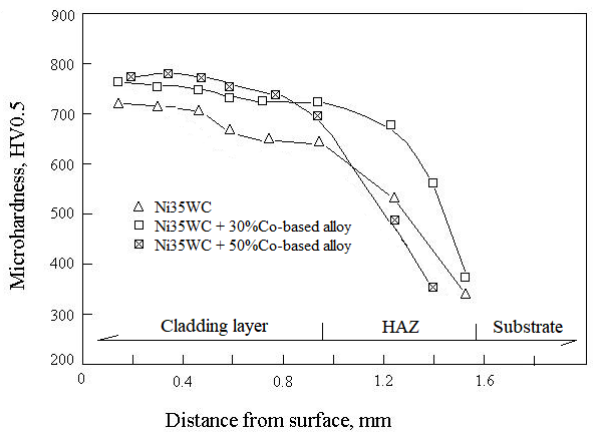

Fig. 5. Sectional hardness gradient curves of laser-clad coatings

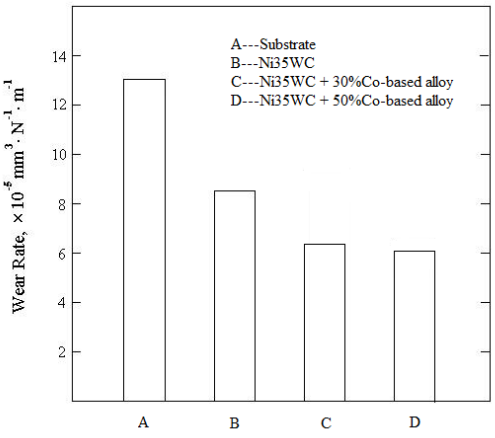

Fig. 6. Wear rate of laser-clad coatings and substrate

The sectional hardness gradient curves of laser-clad Ni35WC, Ni35WC + 30 wt.% Co-based alloy and Ni35WC + 50wt.% Co-based alloy coatings are shown in Fig. 5. When the depth of the cladding layer approaches the bonding zone between the cladding layer and substrate, the hardness of coatings drops sharply to the hardness of substrate. The hardness of Ni35WC coating increases with the additive amount of Co-based alloy powder increased from 30 wt.% to 50 wt.%. In comparison, the hardness range of cladding layers is about 650 – 780 HV, in which the coating with 50 wt.% Co-based alloy has a higher hardness value, about 50 – 100 HV higher than that of the coating without Co-based alloy. The increase of coating hardness is closely related to the addition of Co-based alloy powder and its effect on coating structure.

Fig. 6 shows the comparison of dry sliding wear rates among the substrate and the Ni35WC composite coatings with different Co-based alloy powder content. It can be seen that the wear rate of the laser-clad layer is lower than that of the substrate, and the coating with 50 wt.% Co-based alloy has the lowest wear rate, which reduces the wear rate by about 53 % and 30 % as compared to the substrate and Ni35WC coating, respectively. Therefore, the dry sliding wear resistance of laser cladding Ni35WC + 50 wt.% Co-based alloy coating on stainless steel is significantly improved.

4. DISCUSSION

Based on the microstructural evolution and composition analysis described above, it is inferred that three mechanisms by compositional and microstructural modification play an important role in microstructural refinement and improvement of wear resistance.

First, the fine eutectic phases existing interdendrite of cellular austenite in the coating modified by 50 wt.% Co-based alloy can significantly refine the cellular austenite grains, and the average grain size decreased from ~ 8 μm in Ni35WC coating to ~ 5 μm in 50 wt.% Co alloy coating, the size of the grains in terms of their length and diameter is reduced by almost 50 % (see Fig. 1, Fig. 2). These fine precipitates, which are densely distributed around the austenitic grain boundaries or in the intergranular regions, break the continuity of the austenitic primary crystal growth, and divide some continuous primary crystal into a discontinuous arrangement of cellular grains or discrete isolated grains, and also prevent the growth of some austenitic secondary crystal (see Fig. 2 c, Fig. 4 b). Due to both the strength and toughness of the fine grain structure, grain refinement is considered to be an effective way to improve solidification cracking resistance and mechanical properties [14], and microstructural refinement is also used as a toughening mechanism in laser-deposited Ni-based alloy coatings [23]. In the Ni35WC coating modified by 50 wt.% Co-based alloy, the austenite grains are highly refined and densified, resulting in both strength and toughness improved due to increased grain boundary and dislocation multiplication as well as more uniform plastic deformation among fine grains. Therefore, the microstructural modification not only refined the austenitic dendrite structure, but also improved the hardness and wear resistance of the coatings.

The second important aspect is that the large Cr-rich precipitates in the eutectic region of the Ni35WC coating are refined and the phase type of eutectic structure is changed as a result of disappeared Cr boride brittle phases. Meanwhile，new fine eutectic phases are generated in the modified coating, which makes the interdendritic eutectic structure be changed and refined. The original single Ni-based alloy powder contains a lot of Cr boride and carbide precipitates, such as CrB, Cr_2B, or Cr_7C_3 [26]. In the Ni35WC coating without Co-based alloy, the Cr_7C_3 phase disappears and the Cr_5B_3 phase appears in the XRD pattern, and the precipitates in the interdendritic region are mainly block and lath-shaped Cr-rich phases (see Fig. 3 a, Fig. 4 a). In the Ni35WC coating with 30 wt.% Co-based alloy, the WC phase disappears due to its dissolution completely and a new CrB phase appears in the XRD pattern. The original block and lath-shaped Cr-rich phases are refined into lamellar-shaped phases that existed in the interdendritic region (see Fig. 2 b, Fig. 3 b). When the amount of Co-based alloy powder increases to 50 wt.%, no Cr boride precipitates can be detected from the coating by XRD. A fine grain structure without cracks and pores is obtained, and the eutectic structure is dominated by polymorphous fine precipitates (see Fig. 3 c, Fig. 4 b). If there are more Cr-rich phases in the coating, such as CrB, Cr_2B, Cr_5B_3 or Cr_7C_3, the coating brittleness will be increased, and these brittle phases are prone to fracture under the thermal stress caused by laser cooling, thus forming the sites for crack nucleation and easy routes for crack growth [27]. Because there is no Cr boride brittle phase in the coating modified by 50 wt.% Co-based alloy, and some new fine compounds are formed in the interdendritic region, the phase type of eutectic structure is changed and its structure also refined. As a result, the brittleness of the coating is reduced and the strength and toughness are increased, which will be beneficial to the improvement of the wear resistance of the coating.

The third important role is the contribution of the element Co for the refinement of grains and precipitated phases as well as the improvement of wear resistance. The above two important aspects, such as the austenitic grain refinement, the change of eutectic structure, the formation and precipitation of fine compounds, are related to the effect of Co. It is because of the participation of Co that more Cr-rich phases are formed in the modified coatings. According to the XRD analysis, the diffraction peak intensity from $Cr_{23}C_6$ in the coating with 50 wt.% Co-based alloy is much higher than that of the coating with 30 wt.% Co-based alloy and Ni35WC coating (see Fig. 1, Fig. 2, Fig. 3). Increases in the relative peak intensity of the phase can represent increases in its fraction content. This indicates that a higher volume fraction of $Cr_{23}C_6$ compound is present in the coating due to the addition of more Co-based alloy powder, and the higher content of Co can promote the precipitation of Cr carbide. It is generally believed that $M_{23}C_6$ compounds can be directly formed by combining elements precipitated from supersaturated solid solution with carbon elements, and can also be formed by conversion from other primary phase carbides [28, 29]. EDS analysis (see Table 2) shows that there is a certain amount of Cr, W, and other elements in the γ-Ni solid solution, but no Co, indicating that Co combines with W and C to form Co_6W_6C compound and exists in the eutectic structure. The contents of Cr and W in the solid solution are 21.55 Cr and 28.87 W (wt.%), which are much lower than

32.88 Cr and 46.59 W in the interdendritic region. Thus, although Co did not directly strengthen the solid solution of γ-Ni, it indirectly strengthened the solid solution by reducing the solubility of W and Cr in the solid solution, thereby forming a higher volume fraction of $Cr_{23}C_6$ and $M_{23}(C,B)_6$ compounds in the interdendritic region of Co-modified coatings. High hardness $Cr_{23}C_6$ or $M_{23}(C,B)_6$ compounds and a small amount of Co_6W_6C compound together constitute the main wear-resistant phase, thus increasing the microhardness of the cladding layer and its wear resistance under the dry sliding wear condition. In addition, from the morphological characteristics of the compounds, the morphology of the Cr-rich phase gradually changes from block and lath-shaped to lamellar and thinner lamellar-shaped with the increase of Co content, which indicates that Co can not only promote the precipitation of more Cr-rich phases, but also refine their size. The study by Li et al. [30] on aging alloys also pointed out that Co can increase the nucleation rate and refine the size of precipitates.

From the analysis of the above three aspects, the Ni-Co-W composite coating modified by Co-based alloy can be obtained in the Ni35WC alloy. The coating obtained by compositional and microstructural modifications has the following feature, including the formation of fine cellular austenite crystals, the strengthened solid solution, the eutectic structure altered and refined, the Cr-rich precipitates refined, the brittle phases disappeared, and the coating hardness and wear resistance improved. It can be considered that the improvement of wear resistance of the composite coating is the result of the comprehensive action of solution strengthening, fine grain strengthening, and hard compound diffusion hardening.

5. CONCLUSIONS

The composition and structure of Ni-based alloy with 35 wt.% WC (Ni35WC) were modified by different contents of Co-based alloy powder. The influence of the changes in the composition, microstructure and compounds of the modified coatings on the hardness and dry sliding wear properties has been comparatively investigated by XRD, SEM, and EDS techniques. The following conclusions can be drawn:

1. Co-based alloy can be used to modify the composition and microstructure of Ni35WC alloy. The austenite dendrites in the modified coating with 50 wt.% Co-based alloy is obviously refined. The average size of the cellular grains in terms of their length and diameter is reduced by nearly 50 %, which is beneficial to the improvement of the strength and toughness of the laser-clad layer due to increased grain boundary and dislocation proliferation.
2. The addition of Co-based alloy refines the eutectic compounds in the Ni35WC coating. With the increase of Co-based alloy content, the large Cr-rich phase existing in the austenitic interdendritic region is gradually refined from block and lath-shaped to lamellar and finer lamellar-shaped, and the phase type of eutectic structure is also changed as a result of disappeared Cr boride brittle phases. A large number of fine Cr carbides are formed in the eutectic structure of the coating with 50 wt.% Co-based alloy, so the eutectic structure is changed and refined.
3. By decreasing the solubility of W and Cr in γ-Ni solid solution, element Co resulted in the formation of more volume fraction of $Cr_{23}C_6$ or $M_{23}(C,B)_6$ compounds in the interdendritic region. These fine precipitates are densely distributed around the austenitic grain boundaries or interdendritic region, which prevents grain boundary migration and grain growth by dividing some continuous primary crystal into discrete isolated grains and hindering the growth of some austenitic secondary crystal.
4. The hardness of the coating with 50 wt.% Co-based alloy is about 800 HV, and its dry sliding wear rate reduced by about 53 % and 30 % as compared to the substrate and Ni35WC coating, respectively. It can be considered that the improvement of wear resistance of composite coating is the result of the comprehensive action of solution strengthening, fine grain strengthening, and hard compound diffusion hardening.

REFERENCES

1. **Wang, Y.F., Li, L., Lu, Q.L., Ding, W.T.** Laser Cladding Fe-Based Amorphous Coatings on Stainless Substrate *Chinese Journal of Lasers* 38 (6) 2011: pp. 1 – 4 (in Chinese). https://doi.org/10.3788/CJL201138.0603017
2. **Zhang, D.W., Lei, T.C.** The Microstructure and Erosive-corrosive Wear Performance of Laser Clad Ni-Cr_3C_2 Composite Coating *Wear* 255 (1 – 6) 2003: pp. 129 – 133. https://doi.org/10.1016/S0043-1648(03)00283-7
3. **He, X.M., Liu, X.B., Yang, M.S., Shi, S.H.** Elevated Temperature Tribological Behaviors of Laser Cladding Nickel-Based Composite Coating on Austenitic Stainless Steel *Chinese Journal of Lasers* 38 (9) 2011: pp.1 – 6 (in Chinese). https://doi.org/10.3788/CJL201138.0903007
4. **Zhang, D.W., Zhang, X.P.** Laser Cladding of Stainless Steel with Ni–Cr3C2 and Ni–WC for Improving Erosive–Corrosive Wear Performance *Surface and Coatings Technology* 190(2 – 3) 2005: pp. 212 – 217. https://doi.org/10.1016/j.surfcoat.2004.03.018
5. **Singh, R., Kumar, D., Mishra, S.K., Tiwari, S.K.** Laser Cladding of Stellite 6 On Stainless Steel to Enhance Solid Particle Erosion and Cavitation Resistance *Surface and Coatings Technology* 251 2014: pp. 87 – 97. https://dx.doi.org/10.1016/j.surfcoat.2014.04.008
6. **van der Merwe, J., Tharandt, D.** Corrosion Resistance of Laser Cladded 304L Stainless Steel Enriched with Ru in Hydrochloric Acid *Corrosion Engineering Science and Technology* 52 (1) 2017: pp. 54 – 60. https://doi.org/10.1080/1478422X.2016.1187964
7. **Xu, Z., He, Z., Wang, Z., Zhang, J.** Effects of CeO_2 on the Microstructure and Properties of Laser Cladding 316L Coating *Journal of Materials Engineering and Performance* 28 (8) 2019: pp. 4983 – 4990. https://doi.org/10.1007/s11665-019-04221-w
8. **Wu, G.L., Ren, F.C., Zhang, J., Zhang, Q.L., Liu, R., Yao, J.H.** Microstructure Characteristics and Performance of a Novel Composite Stellite Alloy Fabricated by Laser Cladding *Lasers in Engineering (Old City Publishing)* 42 (4 – 6) 2019: pp. 303 – 321.
9. **Qi, K., Yang, Y., Sun, R., Hu, G.F., Lu, X., Li, J.D., Liang, W.X., Jin, K., Xiong, L.** Effect of Magnetic Field on Crack Control of Co-based Alloy Laser Cladding *Optics*

and Laser Technology 141 2021: pp.107129. https://doi.org/10.1016/j.optlastec.2021.107129

10. **Zhong, M.L., Liu, W.J.** Experimental Research on Cracking Behavior during 45kW High Power CO_2 Laser Cladding *Applied Laser* 19 (5) 1999: pp. 193 – 197 (in Chinese).
11. **Dilawary, S.A.A., Motallebzadeh, A., Atar, E., Cimenoglu, H.** Influence of Mo on the High Temperature Wear Performance of NiCrBSi Hardfacings *Tribology International* 127 2018: pp. 288 – 295. https://doi.org/10.1016/j.triboint.2018.06.022
12. **Korsmik, R., Klimova-Korsmik, O., Valdaytseva, E., Udin, I.** Investigation of Cracking Causes During Multi-Pass Laser Cladding of Heat-Resistant Single Crystal Nickel Alloy *Procedia CIRP* 94 2020: pp. 314 – 319. http://creativecommons.org/licenses/by-nc-nd/4.0/
13. **Griffiths, S., Ghasemi Tabasi, H., Ivas, T., Maeder, X., De Luca, A., Zweiacker, K., Wróbel, R., Jhabvala, J., Logé, R.E., Leinenbach, C.** Combining Alloy and Process Modification for Micro-Crack Mitigation in an Additively Manufactured Ni-Base Superalloy *Additive Manufacturing* 36 2020: pp. 101443. https://doi.org/10.1016/j.addma.2020.101443
14. **Yuan, T., Luo, Z., Kou, S.** Grain Refining of Magnesium Welds by Arc Oscillation *Acta Materialia* 116 2016: pp. 166 – 176. http://dx.doi.org/10.1016/j.actamat.2016.06.036
15. **Foroulis, Z.A.** Guidelines For The Selection of Hardfacing Alloys for Sliding Wear Resistant Applications *Wear* 96 (2) 1984: pp. 203 – 218. https://doi.org/10.1016/0043-1648(84)90094-2
16. **Cubides, Y., Karayan, A.I., Vaughan, M.W., Karaman, I., Castaneda, H.** Enhanced Mechanical Properties and Corrosion Resistance of a Fine-grained Mg-9Al-1Zn Alloy: The Role of Bimodal Grain Structure and β-Mg17Al12 Precipitates *Materialia* 13 2020: pp. 100840. https://doi.org/10.1016/j.mtla.2020.100840
17. **Li, C.L., Park, C.H., Choi, S.W., Lee, S.W., Hong, J.K., Yeom, J.T.** High Strength and High Ductility in The Co-20Cr-15W-10Ni Alloy Having a Bimodal Grain Structure Achieved by Static Recrystallization *Materials Science & Engineering A* 732 2018: pp. 70 – 77. https://doi.org/10.1016/j.msea.2018.06.104
18. **Ueki, K., Yanagihara, S., Ueda, K., Nakai, M., Nakano, T., Narushima, T.** Overcoming the Strength-Ductility Trade-off by the Combination of Static Recrystallization and Low-Temperature Heat-treatment in Co-Cr-W-Ni Alloy for Stent Application *Materials Science & Engineering A* 766 2019: pp. 138400. https://doi.org/10.1016/j.msea.2019.138400
19. **Hou, Q.Y., Huang, Z.Y., Shi, N., Gao, J.S.** Effects of Molybdenum on the Microstructure and Wear Resistance of Nickel-based Hardfacing Alloys Investigated using Rietveld Method *Journal of Materials Processing Technology* 209 (6) 2009: pp. 2767 – 2772. https://doi.org/10.1016/j.jmatprotec.2008.06.025
20. **Dilawary, S.A.A., Motallebzadeh, A., Houdková, S., Medlin, R., Haviar, S., Lukáč, F., Afzal, M., Cimenoglu, H.** Modification of M2 Hardfacing: Effect of Molybdenum Alloying and Laser Surface Melting on Microstructure and Wear Performance *Wear* 404 – 405 2018: pp. 111 – 121. https://doi.org/10.1016/j.wear.2018.03.013
21. **Alhattab, A.A.M., Dilawary, S.A.A., Motallebzadeh, A., Arisoy, C.F., Cimenoglu, H.** Room and High Temperature Sliding Wear Characteristics of Laser Surface Melted Stellite 6 and Mo-Alloyed Stellite 6 Hardfacings (Article) *Journal of Materials Engineering and Performance* 30 (1) 2021: pp. 302 – 311. https://doi.org/10.1007/s11665-020-05375-8
22. **Hemmati, I., Ocelík, V., Th, J., De Hosson, M.** 6 – Compositional modification of Ni-base alloys for laser-deposition technologies *Laser Surface Engineering* 2015: pp. 137 – 162. https://doi.org/10.1016/B978-1-78242-074-3.00006-4
23. **Hemmati, I., Ocelík, V., Th, J., De Hosso, M.** Toughening Mechanism For Ni–Cr–B–Si–C Laser Deposited Coatings *Materials Science and Engineering A* 582 2013: pp. 305 – 315. http://dx.doi.org/10.1016/j.msea.2013.06.010
24. **Liang, C.J., Wang, C.L., Zhang, K.X., Liang, M.L., Xie, Y.G., Liu, W.J., Yang, J.J., Zhou, S.F.** Nucleation and strengthening mechanism of laser cladding aluminum alloy by Ni-Cr-B-Si alloy powder based on rare earth control *Journal of Materials Processing Technology* 294 2021: pp. 117145. https://doi.org/10.1016/j.jmatprotec.2021.117145
25. **Zhao, N., Tao, L., Guo, H., Zhang, M.Q.** Microstructure and Wear Resistance of Laser Cladded Ni-based Coatings with Nanometer La_2O_3 Addition *Rare Metal Materials and Engineering* 46 (8) 2017: pp. 2092 – 2096. https://doi.org/10.1016/S1875-5372(17)30185-6
26. **Li, Q., Zhang, D.W., Lei, T.Q., Chen, C.Z., Chen, W.Z.** Comparison of Laser-Clad and Furnace-Melted Ni-Based Alloy Microstructures *Surface and Coatings Technology* 137 2001: pp. 122 – 135. https://doi.org/10.1016/S0257-8972(00)00732-5
27. **Hemmati, I., Huizeng, R.M., Ocelı´k, V., Th, J., De Hosson, M.** Microstructural Design of Hardfacing Ni–Cr–B–Si–C Alloys *Acta Materialia* 61 2013: pp. 6061 – 6070. http://dx.doi.org/10.1016/j.actamat.2013.06.048
28. **Frenk, A., Kurz, W.** Microstructural Effects on the Sliding Wear Resistance of a Cobalt-Based Alloy *Wear* 174 1994: pp. 81 – 91. https://doi.org/10.1016/0043-1648(94)90089-2
29. **Jiang, W.H., Yao, X.D., Guan, H.R.** Secondary Carbide Precipitation in A Directionally Solidified Cobalt-Base Super-Alloy *Metallurgical and Materials Transactions A* 30A (3) 1999: pp. 513 – 520. https://doi.org/10.1007/s11661-999-0043-7
30. **Li, Z.H., Liu, X.P., Xu, Z.** Influence of W, Co, Ni on Strength and Toughness of Ageing Alloys *The Chinese Journal of Nonferrous Metals* 9 (2) 1999: pp. 236 – 240 (in Chinese). https://doi.org/10.19476/j.ysxb.1004.0609.1999.02.005